

$\rho\gamma^* \rightarrow \pi(\rho)$ transition form factors in the perturbative QCD factorization approach

Ya-Lan Zhang,¹ Shan Cheng,^{2,*} Jun Hua,¹ and Zhen-Jun Xiao^{1,3,†}

¹*Department of Physics and Institute of Theoretical Physics, Nanjing Normal University, Nanjing, Jiangsu 210023, People's Republic of China*

²*Theoretische Elementarteilchenphysik, Naturwissenschaftlich Technische Fakultät, Universität Siegen, 57068 Siegen, Germany*

³*Jiangsu Key Laboratory for Numerical Simulation of Large Scale Complex Systems, Nanjing Normal University, Nanjing 210023, People's Republic of China*

(Received 22 October 2015; published 25 November 2015; corrected 15 March 2016)

In this paper, we studied the $\rho\gamma^* \rightarrow \pi$ and $\rho\gamma^* \rightarrow \rho$ transition processes and made the calculations for the $\rho\pi$ transition form factor $Q^4 F_{\rho\pi}(Q^2)$ and the ρ -meson electromagnetic form factors, $F_{LL,LT,TT}(Q^2)$ and $F_{1,2,3}(Q^2)$, by employing the perturbative QCD (PQCD) factorization approach. For the $\rho\gamma^* \rightarrow \pi$ transition, we found that the contribution to form factor $Q^4 F_{\rho\pi}(Q^2)$ from the term proportional to the distribution amplitude combination $\phi_\rho^T(x_1)\phi_\pi^P(x_2)$ is absolutely dominant, and the PQCD predictions for both the size and the Q^2 -dependence of this form factor $Q^4 F_{\rho\pi}(Q^2)$ agree well with those from the extended anti-de Sitter/QCD models or the light-cone QCD sum rule. For the $\rho\gamma^* \rightarrow \rho$ transition and in the region of $Q^2 \geq 3$ GeV², furthermore, we found that the PQCD predictions for the magnitude and their Q^2 -dependence of the $F_1(Q^2)$ and $F_2(Q^2)$ form factors agree well with those from the QCD sum rule, while the PQCD prediction for $F_3(Q^2)$ is much larger than the one from the QCD sum rule.

DOI: 10.1103/PhysRevD.92.094031

PACS numbers: 12.38.Bx, 12.39.St, 13.40.Gp, 13.66.Bc

I. INTRODUCTION

During the past years, due to its very important role in understanding the hadron structure, the various hadron form factors have been studied intensively for example in Refs. [1–3]. The transition and the electromagnetic form factors of the pseudoscalar mesons, especially the pion meson as the lightest QCD bound state, attracted the most attention theoretically [4–16] and experimentally [17–19]. The transition form factors between the pseudoscalar and vector mesons are also investigated by employing rather different approaches [20–25]; the resulted theoretical predictions, however, are self-consistent and comparable to each other. The radiative form factors of the vector meson, such as the ρ meson, also draw some interest [26,27].

The k_T factorization theorem [28,29] is one of the major factorization approaches based on the factorization hypothesis [30–32] and the resummation image in the end point region [33,34]. Due to its clear advantages, such as no end point singularity and its ability to provide a large strong phase to generate the sizable CP violation for B-meson decays, the perturbative QCD (PQCD) factorization approach based on the k_T factorization theorem has been widely used to study the two-body hadronic decays of $B/B_s/B_C$ mesons for example in Refs. [35–44]. Recently, the next-to-leading-order (NLO) corrections to some important hadron form factors have been calculated [15,45–47]. With the inclusion

of these NLO corrections, the PQCD predictions for the heavy-to-light pseudoscalar form factors in $B \rightarrow \pi$ transition, for example, become well consistent with those from the standard light-meson light-cone QCD sum rule [48–51] and the new B-meson light-cone sum rule [52]. In this paper, we will study the $\rho\pi$ transition form factor and the ρ -meson electromagnetic form factor by employing the PQCD factorization approach.

This paper is organized as follows. The relevant kinetics and the meson wave functions are introduced in Sec. II. In Sec. III, the pseudoscalar and vector transition form factors corresponding to the process $\rho\gamma^* \rightarrow \pi$ are studied with the use of the two-parton meson wave functions up to a subleading twist. In Sec. IV, the ρ -meson electromagnetic form factors in the $\rho\gamma^* \rightarrow \rho$ process are calculated. Section V contains the summary of this paper.

II. KINETICS AND INPUT WAVE FUNCTIONS

In this section, we first consider the relevant kinetics and the input meson wave functions to be used in our calculation. The leading-order (LO) topological diagrams for the meson transition or electromagnetic form factors are presented in Fig. 1. Of course, the full diagrams should also include the other two subdiagrams with the photon vertex being on the lower antiquark lines. Because of the isospin symmetry, these extra two subdiagrams have the same structure as Figs. 1(a) and 1(b) with exchanging the quark and antiquark in the initial and final mesons, and the only difference that may appear is the quark charge.

*cheng@physik.uni-siegen.de
†xiaozenjun@njnu.edu.cn

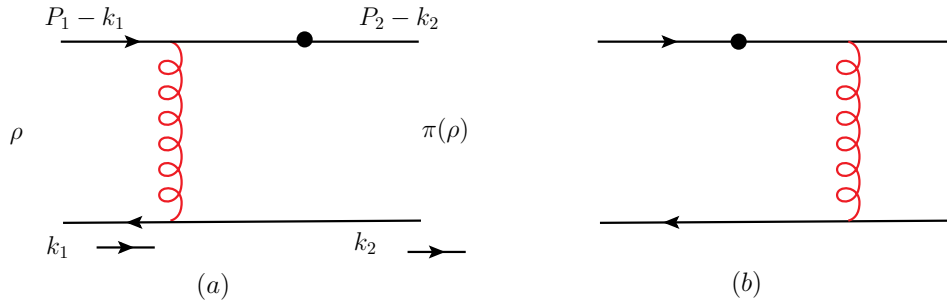


FIG. 1 (color online). The LO diagrams for the $\rho\pi$ transition and ρ -meson electromagnetic form factor, with the symbol \bullet representing the virtual photon vertex.

Under the light-cone (LC) coordinate, the momenta for initial and final mesons in Fig. 1 are defined as

$$P_1 = \frac{Q}{\sqrt{2}}(1, \gamma_{\pi/\rho}^2, \mathbf{0}_T), \quad P_2 = \frac{Q}{\sqrt{2}}(\gamma_{\pi/\rho}^2, 1, \mathbf{0}_T); \\ k_1 = \left(x_1 \frac{Q}{\sqrt{2}}, 0, \mathbf{k}_{1T}\right), \quad k_2 = \left(0, x_2 \frac{Q}{\sqrt{2}}, \mathbf{k}_{2T}\right), \quad (1)$$

where $k_i, i = 1, 2$ is the momentum carried by the antiquark for the initial or final meson with the momentum fraction x_i and \mathbf{k}_{iT} represent the corresponding transversal momentum. The dimensionless parameter $\gamma_\pi^2 \equiv M_\pi^2/Q^2$, $\gamma_\rho^2 \equiv M_\rho^2/Q^2$. Then the momentum transfer squared is $q^2 = (P_1 - P_2)^2 = -Q^2$. The polarization vectors of the initial and final ρ mesons are also defined in the LC coordinate,

$$\epsilon_{1\mu}(L) = \frac{1}{\sqrt{2}\gamma_\rho}(1, -\gamma_\rho^2, \mathbf{0}_T), \quad \epsilon_{1\mu}(T) = (0, 0, \mathbf{1}_T); \\ \epsilon_{2\mu}(L) = \frac{1}{\sqrt{2}\gamma_\rho}(-\gamma_\rho^2, 1, \mathbf{0}_T), \quad \epsilon_{2\mu}(T) = (0, 0, \mathbf{1}_T), \quad (2)$$

with the ρ -meson mass $M_\rho = 0.77$ GeV. The LC definitions in Eq. (1), (2) satisfy the relations

$$P_1 \cdot \epsilon_1 = 0, \quad P_2 \cdot \epsilon_2 = 0; \quad \epsilon_1^2 = \epsilon_2^2 = -1. \quad (3)$$

As elaborated in Ref. [37], the power-suppressed three-parton contribution to the pion electromagnetic form factor in the k_T factorization theorem can only provide $\sim 5\%$ correction to the LO form factor in the whole range of the experimentally accessible momentum transfer squared. This subleading piece amounts only up to few percent of the $B \rightarrow \pi$ transition form factor at a large recoil of the pion in the k_T factorization theorem. So in our calculation for the $\rho\pi$ transition form factor and ρ -meson electromagnetic form factors, we can just consider the dominant contributions from the two-parton meson wave functions and neglect the very small three-parton part safely. The

initial wave functions for transversal and longitudinal polarized ρ meson can be written as

$$\Phi_\rho(P_1, \epsilon_1(L)) = \frac{1}{\sqrt{6}}[\epsilon_1(L)M_\rho\phi_\rho(x_1) + \epsilon_1(L)\not{P}_1\phi_\rho^t(x_1) \\ + M_\rho\phi_\rho^s(x_1)], \quad (4)$$

$$\Phi_\rho(P_1, \epsilon_1(T)) = \frac{1}{\sqrt{6}}[\epsilon_1(T)\not{P}_1\phi_\rho^T(x_1) + \epsilon_1(T)M_\rho\phi_\rho^v(x_1) \\ + iM_\rho\epsilon_{\mu\nu\rho\sigma}\gamma^\mu\gamma_5\epsilon_1^\nu(T)n^\rho v^\sigma\phi_\rho^a(x_1)]. \quad (5)$$

The final pion or rho-meson wave functions are written as

$$\Phi_\pi(P_1) = \frac{1}{\sqrt{6}}[\gamma_5\not{P}_2\phi_\pi^A(x_2) + \gamma_5m_0^\pi\phi_\phi^P(x_2) \\ - \gamma_5m_0^\pi(\not{v}\not{n} - 1)\phi_\pi^T(x_2)]; \quad (6)$$

$$\Phi_\rho(P_2, \epsilon_2(L)) = \frac{1}{\sqrt{6}}[\epsilon_2(L)M_\rho\phi_\rho(x_2) + \epsilon_2(L)\not{P}_2\phi_\rho^t(x_2) \\ + M_\rho\phi_\rho^s(x_2)], \quad (7)$$

$$\Phi_\rho(P_2, \epsilon_2(T)) = \frac{1}{\sqrt{6}}[\epsilon_2(T)\not{P}_2\phi_\rho^T(x_2) + \epsilon_2(T)M_\rho\phi_\rho^v(x_2) \\ + iM_\rho\epsilon_{\mu\nu\rho\sigma}\gamma^\mu\gamma_5\epsilon_2^\nu(T)v^\rho n^\sigma\phi_\rho^a(x_2)]. \quad (8)$$

Here ϕ_π^A , ϕ_ρ^T , and ϕ_ρ are the leading twist-2 (T2) distribution amplitudes (DAs), while $\phi_\pi^{P,T}$, $\phi_\rho^{v,a}$, and $\phi_\rho^{t,s}$ are the subleading twist-3 (T3) DAs which are power suppressed by m_0^π/Q and M_ρ/Q . And m_0^π is the chiral mass of the pion meson.

The pion meson DAs with the inclusion of the high-order effects as given in Ref. [53] are adopted in our numerical calculation,

$$\begin{aligned}
\phi_\pi^A(x) &= \frac{3f_\pi}{\sqrt{6}}x(1-x)[1 + a_2^\pi C_2^{\frac{3}{2}}(t) + a_4^\pi C_4^{\frac{3}{2}}(t)], \\
\phi_\pi^P(x) &= \frac{f_\pi}{2\sqrt{6}} \left[1 + \left(30\eta_3 - \frac{5}{2}\rho_\pi^2 \right) C_2^{\frac{1}{2}}(t) \right. \\
&\quad \left. - 3 \left(\eta_3\omega_3 + \frac{9}{20}\rho_\pi^2(1+6a_2^\pi) \right) C_4^{\frac{1}{2}}(t) \right], \\
\phi_\pi^T(x) &= \frac{f_\pi}{2\sqrt{6}}(1-2x) \\
&\quad \times \left[1 + 6 \left(5\eta_3 - \frac{1}{2}\eta_3\omega_3 - \frac{7}{20}\rho_\pi^2 - \frac{3}{5}\rho_\pi^2 a_2^\pi \right) \right. \\
&\quad \left. \times (1-10x+10x^2) \right], \tag{9}
\end{aligned}$$

where the new Gegenbauer moments a_2^π and a_4^π , the parameters η_3 , ω_3 and ρ_π are the same ones as those defined in Ref. [51]

$$\begin{aligned}
a_2^\pi &= 0.16, & a_4^\pi &= 0.04, & \rho_\pi &= m_\pi/m_0, \\
\eta_3 &= 0.015, & \omega_3 &= -3.0, & & \tag{10}
\end{aligned}$$

with $f_\pi = 0.13$ GeV, $m_\pi = 0.13$ GeV, and $m_\pi^0 = 1.74$ GeV.

For the rho meson, the following twist-2 DAs (ϕ_ρ and ϕ_ρ^T) and twist-3 DAs ($\phi_\rho^{v,a,t,s}$) will be used in our numerical calculation,

$$\begin{aligned}
\phi_\rho(x) &= \frac{3f_\rho}{\sqrt{6}}x(1-x)[1 + a_{2\rho}^{\parallel} C_2^{3/2}(t)], \\
\phi_\rho^T(x) &= \frac{3f_\rho^T}{\sqrt{6}}x(1-x)[1 + a_{2\rho}^{\perp} C_2^{3/2}(t)], \tag{11}
\end{aligned}$$

$$\begin{aligned}
\phi_\rho^v(x) &= \frac{f_\rho}{2\sqrt{6}}[0.75(1+t^2) + 0.24(3t^2-1) \\
&\quad + 0.12(3-30t^2+35t^4)], \\
\phi_\rho^a(x) &= \frac{4f_\rho}{4\sqrt{6}}(1-2x)[1 + 0.93(10x^2-10x+1)]; \\
\phi_\rho^t(x) &= \frac{f_\rho^T}{2\sqrt{6}}[3t^2 + 0.3t^2(5t^2-3) \\
&\quad + 0.21(3-30t^2+35t^4)], \\
\phi_\rho^s(x) &= \frac{3f_\rho^T}{2\sqrt{6}}(1-2x)[1 + 0.76(10x^2-10x+1)], \tag{12}
\end{aligned}$$

where $t = 2x-1$, the Gegenbauer moments $a_{2\rho}^{\parallel} = 0.18$, $a_{2\rho}^{\perp} = 0.2$, and the decay constants $f_\rho = 0.209$, $f_\rho^T = 0.165$. The Gegenbauer polynomials in Eqs. (11) and (12) are of the following form:

$$\begin{aligned}
C_2^{1/2}(t) &= \frac{1}{2}[3t^2-1], \\
C_2^{3/2}(t) &= \frac{3}{2}[5t^2-1], \\
C_4^{1/2}(t) &= \frac{1}{8}[3-30t^2+35t^4], \\
C_4^{3/2}(t) &= \frac{15}{8}[1-14t^2+21t^4]. \tag{13}
\end{aligned}$$

III. $\rho\pi$ TRANSITION FORM FACTOR $Q^4 F_{\rho\pi}(Q^2)$

We first consider the $\rho\gamma^* \rightarrow \pi$ transition; here the two subdiagrams Figs. 1(a) and 1(b) will contribute to the $\rho\pi$ transition form factor. The final state is a pseudoscalar pion meson, which cannot be generated by a scalar current, so only the transversal polarized initial ρ meson with the vector current $J_{\mu,|\lambda|=1}$ contributes to the $\rho\pi$ transition form factor, which can be written as

$$\begin{aligned}
\langle \pi(P_2) | J_\mu | \rho(P_1, \epsilon_1) \rangle &= \langle \pi(P_2) | J_{\mu,|\lambda|=1} | \rho(P_1, \epsilon_1(T)) \rangle \\
&= F_{\rho\pi}(Q^2) \epsilon_{\mu\nu\rho\sigma} \epsilon_1^\nu(T) n^\rho v^\sigma P_1^+ P_2^-.
\end{aligned} \tag{14}$$

For the case of the large momentum transfer, the asymptotic behavior of the hadron form factors is the form of [31]

$$\langle P_2, \lambda_2 | J_\lambda(0) | P_1, \lambda_1 \rangle \sim \left(\frac{1}{\sqrt{|q^2|}} \right)^{|\lambda_1 - \lambda_2| + 2n - 3}. \tag{15}$$

The $\rho\pi$ transition amplitude is suppressed by $1/Q^2$ because of the helicity flipping at the vector vertex for the quark lines ($|\lambda| = 1$). In Eq. (15), λ_1 and λ_2 denote the helicity on the z axis, and n is the parton number of the hadron: when the hadron is a meson, $n = 2$.

From Eqs. (14) and (15), one can see that the $\rho\pi$ transition form factor $F_{\rho\pi}(Q^2)$ has the asymptotic behavior $[Q]^{-4}$ at the limit of large transfer momenta, so one should study the dimensionless form factor $Q^4 F_{\rho\pi}(Q^2)$ rather than $F_{\rho\pi}(Q^2)$ itself. After the inclusion of the contributions from all subdiagrams, Figs. 1(a) and 1(b) and their partner diagrams with the vertexes on the lower antiquark lines, the vector and pseudoscalar $\rho\pi$ transition hard kernel can be written in the following form:

$$\begin{aligned}
&Q^4 H_{\rho\pi}(Q; x_1, x_2; \mathbf{k}_{1T}, \mathbf{k}_{2T}) \\
&= \frac{16\pi\alpha_s}{3} \left\{ \frac{M_\rho [\phi_\rho^v(x_1) - \phi_\rho^a(x_1)] \phi_\pi^A(x_1)}{(P_1 - k_2)^2 (k_1 - k_2)^2} \right. \\
&\quad \left. + \frac{x_1 M_\rho [\phi_\rho^v(x_1) - \phi_\rho^a(x_1)] \phi_\pi^A(x_2) + 2m_\pi^0 \phi_\rho^T(x_1) \phi_\pi^P(x_2)}{(P_2 - k_1)^2 (k_1 - k_2)^2} \right\}.
\end{aligned} \tag{16}$$

By integrating over the longitudinal momentum fractions (x_1, x_2) and the transversal momentum in its conjugate coordinate spaces (b_1, b_2) , we can obtain the $\rho\pi$ transition form factor,

$$\begin{aligned}
Q^4 F_{\rho\pi}(Q^2) = & \frac{16\pi}{3} Q^4 \cdot \alpha_s(\mu) \cdot \int_0^1 dx_1 dx_2 \int_0^\infty b_1 db_1 b_2 db_2 \cdot \exp[-S_{\rho\pi}(x_i, b_i; Q, \mu)] \\
& \times \{M_\rho[\phi_\rho^v(x_1) - \phi_\rho^a(x_1)] \cdot \phi_\pi^A(x_1) \cdot h(x_2, x_1, b_2, b_1) \\
& + x_1 M_\rho[\phi_\rho^v(x_1) - \phi_\rho^a(x_1)] \cdot \phi_\pi^A(x_2) \cdot h(x_1, x_2, b_1, b_2) \\
& + 2m_0^\pi \phi_\rho^T(x_1) \phi_\pi^P(x_2) \cdot S_t(x_1) S_t(x_2) \cdot h(x_1, x_2, b_1, b_2)\},
\end{aligned} \tag{17}$$

where the k_T resummation Sudakov factor $S_{\rho\pi}(x_i, b_i; Q, \mu)$ and the threshold resummation function $S_t(x)$ are the same ones as those being used in Refs. [15,38,47]. The explicit expression of the function $S_{\rho\pi}(x_i, b_i; Q, \mu)$ is of the form

$$S_{\rho\pi}(x_i, b_i, Q, \mu) = s\left(x_i \frac{Q}{\sqrt{2}}, b_i\right) + s\left(\bar{x}_i \frac{Q}{\sqrt{2}}, b_i\right) + 2 \int_{1/b_i}^\mu \frac{d\bar{\mu}}{\bar{\mu}} \gamma_q(g(\bar{\mu})), \tag{18}$$

where $\bar{x}_i = 1 - x_i$ with $i = 1, 2$ for the initial ρ and final π meson, respectively. The expressions of the function $s(Q', b_i)$ and the anomalous dimension $\gamma_q(g(\bar{\mu}))$ can be found in Ref. [54]. For the threshold resummation function $S_t(x)$, it was adopted from Ref. [38]:

$$S_t(x) = \frac{2^{1+2c}\Gamma(3/2+c)}{\sqrt{\pi}\Gamma(1+c)} [x(1-x)]^c; \tag{19}$$

here we set the parameter $c = 0.4$ in the numerical calculations. The hard functions $h(x_1, x_2, b_1, b_2)$ in Eq. (17) come from the Fourier transform of the hard kernel and can be written as [15]

$$\begin{aligned}
h(x_1, x_2, b_1, b_2) = & K_0(\sqrt{x_1 x_2} Q b_2) \\
& \times [\theta(b_1 - b_2) I_0(\sqrt{x_1} Q b_1) \\
& + K_0(\sqrt{x_1} Q b_2) + (b_1 \leftrightarrow b_2)],
\end{aligned} \tag{20}$$

where the functions K_0 and I_0 are the modified Bessel function. Following Refs. [15,38,47], we also choose here μ and μ_f as the largest hard scale in the numerical calculations:

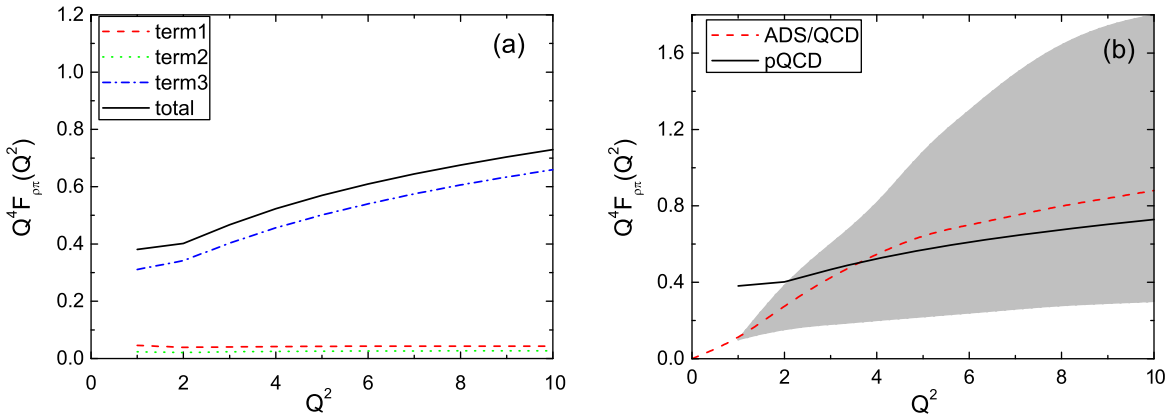


FIG. 2 (color online). (a) the PQCD predictions for the Q^2 -dependence of the $\rho\pi$ transition form factor $Q^4 F_{\rho\pi}(Q^2)$ and (b) the theoretical predictions from AdS/QCD (dashed curve) or the light-cone QCD sum rules (dark region) and from the PQCD factorization approach (solid curve).

- (2) The PQCD predictions for both the magnitude and the Q^2 -dependence of the $\rho\pi$ transition form factor $Q^4 F_{\rho\pi}(Q^2)$ agree well with the theoretical predictions obtained in the extended AdS/QCD models [24] or in the classical light-cone QCD sum rule [9,20,22].

IV. ρ MESON ELECTROMAGNETIC FORM FACTOR $F_i(Q^2)$

In this section, we consider the $\rho\gamma^* \rightarrow \rho$ process and calculate the ρ -meson electromagnetic form factors by employing the PQCD factorization approach. Because the initial and final states are the same ρ meson, we only investigate Fig. 1(a) in detail; the contributions from the other three topological diagrams can be obtained from the exchanging symmetry [15,47] from Fig. 1(a). The lorentz invariant ρ electromagnetic form factors $F_i(Q^2)$, $i = 1, 2, 3$ in the $\rho\gamma^* \rightarrow \rho$ process are defined as the following matrix element [2,27]:

$$\begin{aligned} & \langle \rho(P_2, \epsilon_2^\star) | J_{\mu, \lambda} | \rho(P_1, \epsilon_1) \rangle \\ &= -\epsilon_{2\beta}\epsilon_{1\alpha} \left\{ [(P_1 + P_2)_\mu g^{\alpha\beta} - P_2^\alpha g^{\beta\mu} - P_1^\beta g^{\alpha\mu}] \cdot F_1(Q^2) \right. \\ &\quad \left. - [g^{\mu\alpha} P_1^\beta + g^{\mu\beta} P_2^\alpha] \cdot F_2(Q^2) \right. \\ &\quad \left. + \frac{1}{M_\rho^2} P_2^\alpha P_1^\beta (P_1 + P_2)_\mu \cdot F_3(Q^2) \right\}. \end{aligned} \quad (22)$$

From the asymptotic behavior as defined in Eq. (15), one can see that the transversal form factors are suppressed by $1/Q^2$ or $1/Q^3$,

$$\langle \rho(P_2, \lambda_2 = 0) | J_{\mu, |\lambda|=1} | \rho(P_1, |\lambda_1| = 1) \rangle \sim \frac{1}{Q^2}, \quad (23)$$

$$\langle \rho(P_2, \lambda_2 = \pm 1) | J_{\mu, |\lambda|=0} | \rho(P_1, \lambda_1 = \mp 1) \rangle \sim \frac{1}{Q^3}, \quad (24)$$

while the asymptotic behavior of the longitudinal form factor is the normal one:

$$\langle \rho(P_2, \lambda_2 = 0) | J_{\mu, |\lambda|=0} | \rho(P_1, \lambda_1 = 0) \rangle \sim \frac{1}{Q}. \quad (25)$$

The helicity of the vector current is defined as $\lambda = \lambda_1 + \lambda_2$, and then the transition $\lambda_1 = \pm 1 \rightarrow \lambda_2 = \pm 1$ is forbidden because the helicity of the vector current is $\lambda \leq 1$. The $\lambda_1 = \pm 1 \rightarrow \lambda_2 = 0$ transition in Eq. (23) requires the helicity flipping for one quark line at the vector vertex, which gives a suppression k_T/Q , while the $\lambda_1 = \pm 1 \rightarrow \lambda_2 = \mp 1$ transition in Eq. (24) needs the helicity flipping for both quark lines at the vector vertices, which leads to a suppression k_T^2/Q^2 .

From the radiative matrix element as defined in Eq. (22) and the asymptotic behavior of the hadron form factors as described in Eqs. (23)–(25), we get to know that:

- (i) Only the electric form factor $F_1(Q^2)$ contributes to the transversal form factor $F_{\text{TT}}(Q^2)$ with $\lambda_1 = -\lambda_2 = \pm 1$.
- (ii) Both the electric form factor $F_1(Q^2)$ and the magnetic form factor $F_2(Q^2)$ contribute to the semitransversal form factor F_{LT} with $\lambda_i = \pm 1$ & $\lambda_j = 0$ ($i, j = 1, 2, i \neq j$);
- (iii) All $F_1(Q^2)$, $F_2(Q^2)$, and the quadruple form factor $F_3(Q^2)$ give the contribution to the longitudinal radiation form factor F_{LL} with $\lambda_1 = \lambda_2 = 0$.

These form factors do satisfy the following relations by definition:

$$\begin{aligned} F_{\text{TT}}(Q^2) &= F_1(Q^2), \\ F_{\text{LT}}(Q^2) &= \frac{Q}{2M_\rho} [F_1(Q^2) + F_2(Q^2)], \\ F_{\text{LL}}(Q^2) &= F_1(Q^2) - \frac{Q^2}{2M_\rho^2} F_2(Q^2) \\ &\quad + \frac{Q^2}{M_\rho^2} \left(1 + \frac{Q^2}{4M_\rho^2} \right) F_3(Q^2). \end{aligned} \quad (26)$$

By introducing the transversal momentum k_T to cancel the end point singularity, integrating over the longitudinal momentum fractions and transversal coordinate conjugated to transversal momentum, one finds the PQCD predictions for the Q^2 -dependence of the ρ -meson electromagnetic form factors,

$$\begin{aligned} F_{\text{LL}}(Q^2) &= \frac{32\pi C_F}{3} Q^2 \alpha_s(\mu) \int_0^1 dx_1 dx_2 \int_0^\infty b_1 db_1 b_2 db_2 \cdot \exp[-S_\rho(x_i; b_i; Q; \mu)] \left\{ \left[x_2 - \frac{1}{2} \gamma_\rho^2 (1 + x_2) \right] \phi_\rho(x_1) \phi_\rho(x_2) \right. \\ &\quad \left. + \gamma_\rho^2 \phi_\rho^s(x_1) \phi_\rho^t(x_2) + 2\gamma_\rho^2 (1 - x_2) \phi_\rho^s(x_1) \phi_\rho^s(x_2) \right\} \cdot h(x_2, x_1, b_2, b_1), \end{aligned} \quad (27)$$

$$\begin{aligned} F_{\text{LT}}(Q^2) &= \frac{32\pi C_F}{3} Q M_\rho \alpha_s(\mu) \int_0^1 dx_1 dx_2 \int_0^\infty b_1 db_1 b_2 db_2 \cdot \exp[-S_\rho(x_i; b_i; Q; \mu)] \\ &\quad \times \left\{ \frac{1}{2} [\phi_\rho^v(x_1) + \phi_\rho^a(x_1)] \phi_\rho(x_2) + \phi_\rho^s(x_1) \phi_\rho^T(x_2) - \frac{1}{2} x_2 \phi_\rho(x_1) [\phi_\rho^v(x_2) + \phi_\rho^a(x_2)] \right\} \cdot h(x_2, x_1, b_2, b_1), \end{aligned} \quad (28)$$

$$F_{\text{TT}}(Q^2) = \frac{32\pi C_F}{3} M_\rho^2 \alpha_s(\mu) \int_0^1 dx_1 dx_2 \int_0^\infty b_1 db_1 b_2 db_2 \cdot \exp[-S_\rho(x_i; b_i; Q; \mu)] \\ \times \{(1-x_2)[\phi_\rho^a(x_1)\phi_\rho^a(x_2) - \phi_\rho^v(x_1)\phi_\rho^v(x_2)] \\ + (1+x_2)[\phi_\rho^a(x_1)\phi_\rho^v(x_2) - \phi_\rho^v(x_1)\phi_\rho^a(x_2)]\} \cdot h(x_2, x_1, b_2, b_1), \quad (29)$$

where $C_F = 4/3$ and the Sudakov factor $S_\rho(x_i; b_i; Q; \mu)$ and the hard function $h(x_2, x_1, b_2, b_3)$ are the same ones as those in Eqs. (17), (18), and (20). With these form factors of different polarized initial and final states and the relations in Eq. (26), one can obtain easily the Q^2 -dependence of Lorentz-invariant electric, magnetic, and quadrupole form factors $F_1(Q^2)$, $F_2(Q^2)$, and $F_3(Q^2)$.

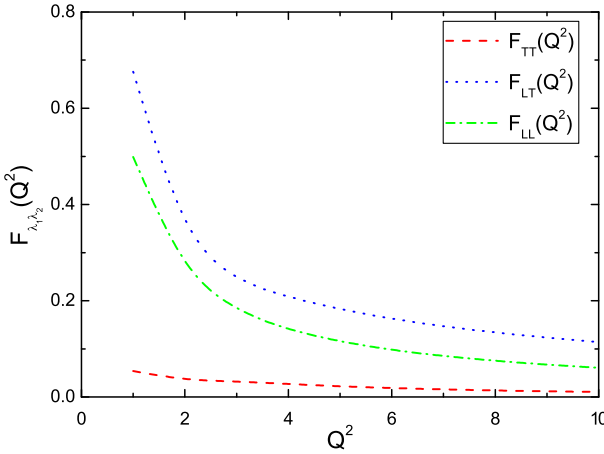


FIG. 3 (color online). The PQCD predictions for Q^2 dependence of the ρ -meson form factors $F_{\lambda_1\lambda_2}(Q^2)$ with different polarizations for initial and final states. The short dashed, dots, and dot-dashed curves represent the form factors $F_{\text{TT}}(Q^2)$, $F_{\text{LT}}(Q^2)$, and $F_{\text{LL}}(Q^2)$, respectively.

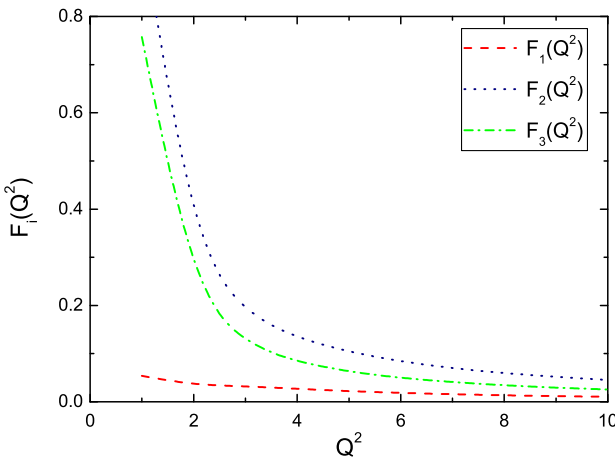


FIG. 4 (color online). The PQCD predictions for Q^2 -dependence of the Lorentz-invariant ρ -meson electromagnetic form factors $F_{1,2,3}(Q^2)$. The short dashed, dots, and dot-dashed curves represent the electric [$F_1(Q^2)$], the magnetic [$F_2(Q^2)$], and the quadrupole [$F_3(Q^2)$] form factors, respectively.

The PQCD predictions for the Q^2 -dependence of the ρ -meson electromagnetic form factors with different polarizations [i.e., $F_{\text{LL}}(Q^2)$, $F_{\text{LT}}(Q^2)$, and $F_{\text{LL}}(Q^2)$] are presented in Fig. 3, while the Q^2 -dependence of the ρ -meson electric, magnetic, and quadrupole form factors with different Lorentz structures [i.e., $F_{1,2,3}(Q^2)$] are presented in Fig. 4. From these two figures, one can find the following points:

- (i) For the form factors with different polarizations, there exists an approximate relation: $F_{\text{LT}}(Q^2) \gtrsim F_{\text{LL}}(Q^2) \gg F_{\text{TT}}(Q^2)$. The asymptotic behavior displayed in Eq. (15) is partially violated for $F_{\text{LT}}(Q^2)$ and $F_{\text{LL}}(Q^2)$. This violation arises because the longitudinal form factor F_{LL} has an additional suppression from x_2 , although its asymptotic behavior has a Q/M_ρ enhancement when compared to the semitransversal form factor F_{LT} . And this violation is consistent with the light-cone sum rule result [2].
- (ii) The value of the electric form factor $F_1(Q^2)$ is rather small, because it is equal to the heavily suppressed transversal form factor $F_{\text{TT}}(Q^2)$ as defined in Eq. (26). In the region of $Q^2 \geq 3 \text{ GeV}^2$, there exists also an approximate relation for the values of $F_{1,2,3}(Q^2)$: $F_2(Q^2) \gtrsim F_3(Q^2) \gtrsim F_1(Q^2)$. Our PQCD predictions for $F_1(Q^2)$ and $F_2(Q^2)$ form factors agree well with the QCD sum rule results [27] in the region $Q^2 \geq 3 \text{ GeV}^2$. But the PQCD prediction for the quadrupole form factor $F_3(Q^2)$ is much larger than the one from the QCD sum rule, the hierarchy $F_1(Q^2) \gg F_3(Q^2)$ between $F_1(Q^2)$ and $F_3(Q^2)$ predicted in the QCD sum rule [27] is therefore changed here.

V. SUMMARY

By employing the PQCD factorization approach, we studied the $\rho\gamma^* \rightarrow \pi$ and the $\rho\gamma^* \rightarrow \rho$ transition processes and made the analytical and numerical evaluations for the $\rho\pi$ transition form factor $Q^4 F_{\rho\pi}(Q^2)$ and the ρ -meson electromagnetic form factors, $F_{\text{LL,LT,TT}}(Q^2)$ and $F_{1,2,3}(Q^2)$. We found the following results:

- (i) For the $\rho\gamma^* \rightarrow \pi$ transition process, the contribution to the $\rho\pi$ transition form factor $Q^4 F_{\rho\pi}(Q^2)$ from the terms proportional to the DAs combination $\phi_\rho^T(x_1)\phi_\pi^P(x_2)$ is absolutely dominant, and the PQCD predictions for both the magnitude and the Q^2 -dependence of this form factor agree well with those from the extended AdS/QCD models or from the light-cone QCD sum rule.

- (ii) For the $\rho\gamma^* \rightarrow \rho$ transition process and in the region of $Q^2 \geq 3$ GeV 2 , we found that the PQCD predictions for the magnitude and their Q^2 -dependence of the $F_1(Q^2)$ and $F_2(Q^2)$ form factors agree well with those from the QCD sum rule, while the PQCD prediction for the quadruple $F_3(Q^2)$ is much larger than the one from the QCD sum rule.

ACKNOWLEDGMENTS

The authors would like to thank Hsiang-nan Li and Cai-Dian Lü for valuable discussions. This work is supported by the National Natural Science Foundation of China under Grant No. 11235005 and by the Project on Graduate Students Education and Innovation of Jiangsu Province under Grant No. KYZZ15-0212.

-
- [1] A. I. Vainshtein and V. I. Zakharov, *Phys Lett. B* **72**, 368 (1978); R. G. Arnold, C. E. Carlson, and F. Gross, *Phys. Rev. C* **21**, 1426 (1980).
- [2] B. L. Ioffe and A. V. Smilga, *Nucl. Phys. B* **216**, 373 (1983).
- [3] H. M. Choi and C. R. Ji, *Nucl. Phys. A* **618**, 291 (1997); P. Maris and P. C. Tandy, *Phys. Rev. C* **65**, 045211 (2002); R. G. Edwards, *Nucl. Phys. B*, *Proc. Suppl.* **140**, 290 (2005).
- [4] A. V. Efremov and A. V. Radyushkin, *Phys. Lett.* **94B**, 245 (1980).
- [5] B. Melic, B. Nizic, and K. Passek, *Phys. Rev. D* **60**, 074004 (1999).
- [6] A. P. Bakulev, K. Passek-Kumericki, W. Schroers, and N. G. Stefanis, *Phys. Rev. D* **70**, 033014 (2004).
- [7] C. E. Carlson and J. Milana, *Phys. Rev. Lett.* **65**, 1717 (1990).
- [8] V. A. Nesterenko and A. V. Radyushkin, *Phys. Lett. B* **115**, 410 (1982).
- [9] V. Braum and I. Halperin, *Phys. Lett. B* **328**, 457 (1994).
- [10] A. Khodjamirian, Report No. WUE-ITP-99-021; V. M. Braun, A. Khodjamirian, and M. Maul, *Phys. Rev. D* **61**, 073004 (2000); J. Bijnens and A. Khodjamirian, *Eur. Phys. J. C* **26**, 67 (2002).
- [11] U. Raha and A. Aste, *Phys. Rev. D* **79**, 034015 (2009).
- [12] F. D. R. Bonnet, R. G. Edwards, G. T. Fleming, R. Lewis, and D. G. Richards, *Phys. Rev. D* **72**, 054506 (2005); G. T. Fleming, F. D. R. Bonnet, R. G. Edwards, R. Lewis, and D. G. Richards, *Nucl. Phys. B*, *Proc. Suppl.* **140**, 302 (2005).
- [13] E. R. Arriola and W. Broniowski, *Phys. Rev. D* **74**, 034008 (2006).
- [14] S. V. Mikailov and N. G. Stefanis, *Nucl. Phys. B* **821**, 291 (2009).
- [15] H. N. Li, Y. L. Shen, Y. M. Wang, and H. Zou, *Phys. Rev. D* **83**, 054029 (2011); S. Cheng, Y. Y. Fan, and Z. J. Xiao, *Phys. Rev. D* **89**, 054015 (2014).
- [16] H. N. Li, Y. L. Shen, and Y. M. Wang, *J. High Energy Phys.* **01** (2014) 004.
- [17] C. J. Bebek, C. N. Brown, and M. Herzlinger *et al.*, *Phys. Rev. D* **9**, 1229 (1974); C. J. Bebek, C. N. Brown, and S. D. Holmes *et al.*, *Phys. Rev. D* **17**, 1693 (1978).
- [18] T. Horn *et al.* (Jefferson Lab F_π Collaboration), *Phys. Rev. Lett.* **97**, 192001 (2006).
- [19] T. K. Pedlar *et al.* (CLEO Collaboration), *Phys. Rev. Lett.* **95**, 261803 (2005).
- [20] V. L. Eletsky and Y. I. Kogan, *Z. Phys. C* **20**, 357 (1983).
- [21] J. H. Yu, B. W. Xiao, and B. Q. Ma, *J. Phys. G* **34**, 1845 (2007).
- [22] A. Khodjamirian, *Eur. Phys. J. C* **6**, 477 (1999).
- [23] A. Gökalp and O. Yilmaz, *Eur. Phys. J. C* **24**, 117 (2002).
- [24] F. Zuo, Y. Jia, and T. Huang, *Eur. Phys. J. C* **67**, 253 (2010) and references therein.
- [25] C. D. Lü, W. Wang, and Y. M. Wang, *Phys. Rev. D* **75**, 094020 (2007).
- [26] S. L. Zhu, W.-Y. P. Hwang, and Z. S. Yang, *Phys. Lett. B* **420**, 8 (1998); S. J. Brodsky and J. R. Hiller, *Phys. Rev. D* **46**, 2141 (1992); H. M. Choi and C. R. Ji, *Phys. Rev. D* **70**, 053015 (2004); T. M. Aliev and M. Savci, *Phys. Rev. D* **70**, 094007 (2004).
- [27] V. V. Braguta and A. I. Onishchenko, *Phys. Rev. D* **70**, 033001 (2004).
- [28] S. J. Brodsky and G. R. Farrar, *Phys. Rev. Lett.* **31**, 1153 (1973); J. Botts and G. Sterman, *Nucl. Phys. B* **325**, 62 (1989); S. J. Brodsky, C. R. Ji, A. Pang, and D. G. Robertson, *Phys. Rev. D* **57**, 245 (1998); H. N. Li and G. Sterman, *Nucl. Phys. B* **381**, 129 (1992); T. Huang and Q. X. Shen, *Z. Phys. C* **50**, 139 (1991).
- [29] M. Nagashima and H. N. Li, *Phys. Rev. D* **67**, 034001 (2003).
- [30] G. P. Lepage and S. J. Brodsky, *Phys. Rev. D* **22**, 2157 (1980).
- [31] V. L. Chernyak and A. R. Zhitnitsky, *Phys. Rep.* **112**, 173 (1984).
- [32] G. P. Lepage and S. J. Brodsky, *Phys. Rev. Lett.* **43**, 545 (1979); *Phys. Rev. D* **22**, 2157 (1980).
- [33] T. Hyer, *Phys. Rev. D* **47**, 3875 (1993).
- [34] H. N. Li, *Phys. Rev. D* **66**, 094010 (2002); *Phys. Lett. B* **555**, 197 (2003).
- [35] F. G. Cao, T. Huang, and C. W. Luo, *Phys. Rev. D* **52**, 5358 (1995).
- [36] Z. T. Wei and M. Z. Yang, *Phys. Rev. D* **67**, 094013 (2003).
- [37] Y. C. Chen and H. N. Li, *Phys. Rev. D* **84**, 034018 (2011); Y. C. Chen and H. N. Li, *Phys. Lett. B* **712**, 63 (2012).
- [38] T. Kurimoto, H. N. Li, and A. I. Sanda, *Phys. Rev. D* **65**, 014007 (2001); M. Nagashima and H. N. Li, *Eur. Phys. J. C* **40**, 395 (2005).
- [39] C. D. Lü, K. Ukai, and M. Z. Yang, *Phys. Rev. D* **63**, 074009 (2001); C. D. Lü and M. Z. Yang, *Eur. Phys. J. C* **28**, 515 (2003).
- [40] T. Huang and X. G. Wu, *Phys. Rev. D* **70**, 093013 (2004).

- [41] X. Liu, H. S. Wang, Z. J. Xiao, and L. B. Guo, *Phys. Rev. D* **73**, 074002 (2006); H. S. Wang, X. Liu, Z. J. Xiao, L. B. Guo, and C. D. Lü, *Nucl. Phys. B* **738**, 243 (2006); Z. T. Zou and C. D. Lü, *Chin. Sci. Bull.* **59**, 3738 (2014).
- [42] Y. Li, C. D. Lü, Z. J. Xiao, and X. Q. Yu, *Phys. Rev. D* **70**, 034009 (2004); Z. J. Xiao, X. Liu, and H. S. Wang, *Phys. Rev. D* **75**, 034017 (2007); A. Ali, G. Kramer, Y. Li, C. D. Lü, Y. L. Shen, W. Wang, and Y. M. Wang, *Phys. Rev. D* **76**, 074018 (2007); Z. J. Xiao, W. F. Wand, and Y. Y. Fan, *Phys. Rev. D* **85**, 094003 (2012); X. Liu, H. N. Li, and Z. J. Xiao, *Phys. Rev. D* **86**, 011501(R) (2012).
- [43] X. Liu, Z. J. Xiao, and C. D. Lü, *Phys. Rev. D* **81**, 014022 (2010); X. Liu and Z. J. Xiao, *Phys. Rev. D* **81**, 074017 (2010); X. Liu and Z. J. Xiao, *Phys. Rev. D* **82**, 054029 (2010); Z. J. Xiao and X. Liu, *Chin. Sci. Bull.* **59**, 3748 (2014).
- [44] J. J. Wang, D. T. Lin, W. Sun, Z. J. Ji, S. Cheng, and Z. J. Xiao, *Phys. Rev. D* **89**, 074046 (2014); Y. L. Zhang, X. Y. Liu, Y. Y. Fan, S. Cheng, and Z. J. Xiao, *Phys. Rev. D* **90**, 014029 (2014); Y. Y. Fan, W. F. Wang, S. Cheng, and Z. J. Xiao, *Chin. Sci. Bull.* **59**, 125 (2014); Z. J. Xiao, Y. Y. Fan, W. F. Wang, and S. Cheng, *Chin. Sci. Bull.* **59**, 3787 (2014).
- [45] H. N. Li, Y. L. Shen, and Y. M. Wang, *Phys. Rev. D* **85**, 074004 (2012); S. Cheng, Y. Y. Fan, X. Yu, C. D. Lü, and Z. J. Xiao, *Phys. Rev. D* **89**, 094004 (2014).
- [46] H. C. Hu and H. N. Li, *Phys. Lett. B* **718**, 1351 (2013); S. Cheng and Z. J. Xiao, *Phys. Lett. B* **749**, 1 (2015).
- [47] S. Cheng, Y. L. Zhang, and Z. J. Xiao, *Nucl. Phys. B* **896**, 255 (2015).
- [48] V. M. Belyaev, A. Khodjamirian, and R. Rückl, *Z. Phys. C* **60**, 349 (1993).
- [49] P. Ball and R. Zwicky, *Phys. Rev. D* **71**, 014015 (2005).
- [50] A. Khodjamirian, T. Mannel, N. Offen, and Y. M. Wang, *Phys. Rev. D* **83**, 094031 (2011).
- [51] G. Duplančić, A. Khodjamirian, Th. Mannel, B. Melić, and N. Offen, *J. High Energy Phys.* **04** (2008) 014.
- [52] Y. M. Wang and Y. L. Shen, *Nucl. Phys. B* **898**, 563 (2015).
- [53] P. Ball, *J. High Energy Phys.* **01** (1999) 010; P. Ball, V. M. Braun, Y. Koike, and K. Tanaka, *Nucl. Phys. B, Proc. Suppl.* **529**, 323 (1998); P. Ball, V. M. Braun, and A. Lenz, *J. High Energy Phys.* **05** (2006) 004; P. Ball and R. Zwicky, *Phys. Rev. D* **71**, 014015 (2005).
- [54] H. N. Li and B. Tseng, *Phys. Rev. D* **57**, 443 (1998).